Article

Journal of
Nanoscience and Nanotechnology
Vol. 15, 1030–1036, 2015
www.aspbs.com/jnn

Structure and Bonding in Chlorine-Functionalized Nanodiamond—Nuclear Magnetic Resonance and X-Ray Photoelectron Spectroscopy Study

Alexander M. Panich[1,*], Nikolay A. Sergeev[2], Marcin Olszewski[2], Natalya Froumin[3], Arthur T. Dideykin[4], Vasiliy V. Sokolov[4], and Alexander Ya. Vul'[4]

[1] *Department of Physics, Ben-Gurion University of the Negev, P.O. Box 653, Be'er Sheva 84105, Israel*
[2] *Institute of Physics, University of Szczecin, 70-451 Szczecin, Poland*
[3] *Ilse Katz Institute for Nanoscale Science and Technology, Ben-Gurion University of the Negev, P.O. Box 653, Be'er Sheva 84105, Israel*
[4] *Ioffe Physical-Technical Institute, Polytechnicheskaya 26, St. Petersburg 194021, Russia*

We report on investigation of detonation nanodiamond annealed at 800 °C in chlorine atmosphere by means of ^{1}H, ^{13}C and ^{35}Cl nuclear magnetic resonance and X-ray photoelectron spectroscopy. The results of these methods are found to be consistent with each other and evidence formation of chlorine-carbon groups and sp^2 carbon shell on the nanodiamond surface. The data obtained provide detailed information about the structure and bonding in this diamond nanoparticle. Interaction of nuclear spins with unpaired electron spins of dangling bonds results in fast ^{13}C nuclear spin-lattice relaxation.

Keywords: Diamond Nanoparticles, Chlorine, NMR, XPS.

1. INTRODUCTION

Diamond nanoparticles have risen to the forefront of materials research over the last two decades due to great potential for a variety of materials and biomedical applications.[1–8] These materials are mainly fabricated by detonation technique accompanied by a subsequent purification, allowing industrial production of the diamond nanoparticles. The resulting product is called detonation nanodiamond (DND). Substantial technological progress has recently been achieved in preparation hydrosols of mono-dispersed nanodiamond particles with narrow size distribution, having maximum around 4 nm.[9–11] The DND particle consists of a mechanically stable and chemically inert diamond core and chemically active surface, which can be easily modified with a variety of techniques. Purposeful functionalization of the DND surface with targeted species and functional groups[12–18] allows controllable preparation of DNDs with specified chemical, physical, and electronic properties. Due to their high biocompatibility and non-toxicity, nanodiamonds are promising multi-functional systems for medical applications, such as drug delivery, cancer therapeutics, microbiological fluorescence probes and biomarkers. For *in vivo* drug delivery, the surface charge of NDs must be controlled without size increase. Moreover, surface functional groups are essential to provide specific properties in physiological media such as stability and solubility.

An important stage in solving the problems of the biomedical applications of DNDs is a detailed characterization of the surface after its coating and grafting by different physical methods that are sensitive to the chemical structure and bonding and can distinguish between different functional groups. For this purpose, the most useful and frequently used are spectroscopic methods such as nuclear magnetic resonance (NMR), electron paramagnetic resonance (EPR), X-ray photoelectron spectroscopy (XPS), infra-red (IR) and Raman spectroscopy.[12–29]

In the present paper, we report on our ^{1}H, ^{13}C and ^{35}Cl NMR and XPS investigation of detonation nanodiamond, whose surface was modified by annealing at 800 °C in chlorine atmosphere (hereafter called Cl-DND). Such a material is of interest since halogenation leads to an activation of the nanodiamond surface, making it capable of further functionalization and conjugation of therapeutic

*Author to whom correspondence should be addressed.

1533-4880/2015/15/1030/007 doi:10.1166/jnn.2015.9737

materials, thus expanding eventual biomedical applications of NDs (Refs. [13, 30] and references therein). The results of the above-mentioned methods are found to be consistent with each other and evidence formation of chlorine-carbonic groups and sp^2 carbon spots on the nanodiamond surface. The data obtained provide detailed information about the structure and bonding in such diamond nanoparticles. The sample reveals a significant number of paramagnetic defects (1.44×10^{20} spin/g compared to $N_s = 6.3 \times 10^{19}$ spins/g in well-purified nanodiamonds[20]), resulting in fast ^{13}C nuclear spin-lattice relaxation.

2. EXPERIMENTAL DETAILS

Initial DND sample was prepared by dry synthesis, carefully purified from metallic magnetic impurities in potassium bichromate and hydrochloric acid. Then the powder sample was annealed in chlorine atmosphere at 800 °C to receive Cl-DND compound under study. The processing was carried out in a flow reactor (electric furnace with a tubular graphitic heater, into which the nanodiamond sample was placed). Heating to a desired temperature was held in a flow of Argon, which was then replaced by gaseous Cl_2. Specific Cl_2 flow was 0.5 liter/min, the treatment time was 30 min. Cooling of the sample was done in Argon flow with a specific flow rate of 0.5 liter/min for 40 min. The mass loss was 14.7%, herewith the powder changed its color from grey to black. The composition of initial and chlorine-modified samples, measured by energy dispersive analysis using Quanta 200 microscope equipped with EDAX attachment, is shown in Table I. The chemical treatment used in this work yields stable material, though, as one can find from Table I, only partial chlorination of the ND surface is obtained. The received chlorine content (4.18 at. %, which corresponds to 11.3 wt. %), is much larger than 2.9 wt. % achieved in Ref. [30] after 8 h of photochemical chlorination of nanodiamond. However, it is twice less than 8.6 at. % obtained for nanodiamond fluorination by a mixture of fluorine and hydrogen gases in the temperature range 150 to 470 °C for 48 h.[13] Such a difference may presumably be attributed to higher electronegativity and reactivity of fluorine comparing to chlorine.

Static and magic angle spinning (MAS) ^{13}C and ^{1}H nuclear magnetic resonance (NMR) spectra, spin-lattice (T_1) and spin–spin (T_2) relaxation times have been measured at room temperature using FT-NMR Bruker Avance III™ 400 MHz WB and Tecmag Libra 340 MHz spectrometers equipped by superconducting magnets.

Table I. Composition of initial and chlorine-modified samples.

	Composition, at. %						
	C	O	Al	Cl	Cr	Ni	S
Initial sample	92.26	7.56	0.07	0.06	0.05	–	–
Chlorine-modified sample	95.40	0.18	0.04	4.18	–	0.18	0.02

The measurements were made in the applied magnetic fields $B_0 = 9.398$ and 8.0196 T, corresponding to ^{1}H resonance frequencies of 400.15 and 341.44 MHz and ^{13}C resonance frequencies of 100.62 and 85.86 MHz, respectively. MAS measurements were carried out with 2.5 mm rotor at spinning rate 30 kHz. Static room temperature ^{35}Cl NMR spectrum was measured in an applied magnetic field $B_0 = 7.99946$ T at a resonance frequency of 33.38 MHz. ^{13}C and ^{1}H chemical shifts are given relative to ^{13}C and ^{1}H resonances in tetramethylsilane (TMS) at 0 ppm. ^{35}Cl chemical shift is given relative to 0.1 mol solution of NaCl in D_2O at 0 ppm. The spin-lattice relaxation time T_1 was measured using a saturation-comb sequence. The spin–spin relaxation time T_2 was measured using the 2D set of nuclear spin echo signals with a variable delay between pulses. T_2 was determined using a plot of the decaying echo amplitude as the point at which this amplitude falls to 1/e of its initial value.

X-ray photoelectron spectroscopy (XPS) spectra were measured using ESCALAB 250 spectrometer with Al X-ray source and monochromator. Calibration was performed according to the position of the Au 4f7 line. General survey and high-resolution spectra of elements were recorded.

Room temperature ($T = 295$ K) electron paramagnetic resonance (EPR) measurement was done using a Bruker EMX-220 X-band ($\nu = 9.4$ GHz) spectrometer. This measurement reveals density of paramagnetic defects $N_s = 1.44 \times 10^{20}$ spin/g.

3. RESULTS AND DISCUSSION

3.1. ^{13}C NMR Spectra, Spin-Lattice and Spin–Spin Relaxation

The static ^{13}C NMR spectrum of the Cl-DND (Fig. 1) can be deconvoluted into two components. An intense narrow signal with a chemical shift $\sigma(^{13}C) = 35 \pm 1$ ppm is characteristic of bulk diamond[18, 31–33] and is attributed to the

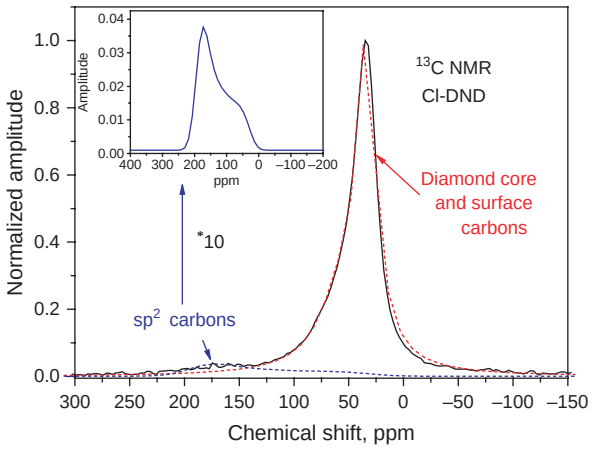

Figure 1. Static ^{13}C spectrum of Cl-DND (102400 scans, recycle delay 1 s). Deconvolution into two components is shown by dashed lines.

sp^3-carbons of the nanodiamond core and to the surface carbon atoms with sp^3 hybridization. The second component reveals a broad asymmetric line characteristic of axially symmetric chemical shielding tensor with the center of gravity at $\sigma_{iso} \approx 130$ ppm and $\Delta\sigma = \sigma_{\parallel} - \sigma_{\perp} \approx 160$ ppm; the maximum of this spectrum is positioned at $\sigma_{\perp} \approx 180$ ppm. This component is characteristic of aromatic carbons and is attributed to graphitic-like carbon atoms at the surface of the diamond core. (For comparison, bulk graphite reveals $\sigma_{iso} = 119$ ppm and $\Delta\sigma = 178$ ppm[34]).

More detailed information comes from the ^{13}C NMR measurement of the Cl-DND sample using magic angle spinning (MAS) at the spinning rate of 30 kHz, which averages anisotropic interactions of nuclear spins and yields well-resolved lines positioned at their centers of gravities (σ_{iso}). One can find from Figure 2 that the ^{13}C MAS spectrum reveals three components. An intense narrow signal with a chemical shift $\sigma(^{13}C) = 35$ ppm is attributed to the sp^3-carbons of the nanodiamond core. A weak component at $\sigma(^{13}C) = 50$ ppm is assigned to carbon atoms involved into the C—Cl bonds. The chemical shift of the third component, $\sigma(^{13}C) = 124$ ppm, is characteristic of aromatic sp^2 carbons and is attributed to a graphene-like shell that covers the diamond core. This finding clearly indicates graphitization of the diamond surface and formation of the covalently bound chlorine-carbon groups under annealing at 800 °C in the chlorine atmosphere. One can find from the line intensities that the sp^3 carbons, C—Cl bound carbons and sp^2 carbons account for 68, 3 and 29% of all carbons, respectively. While the sp^2 shell is nearly not apparent in the ^{13}C MAS spectrum of the initial sample,[35,36] in the annealed chlorinated compound it is large enough to cover the 4.5 nm nanodiamond particle by 1.5–2 layers of graphene-like shell. This finding correlates well with our recent ^{13}C NMR study,[36] which shows that sp^3-to-sp^2 transformation under annealing of nanodiamond in vacuum starts at temperatures above 600 °C, and that graphitization

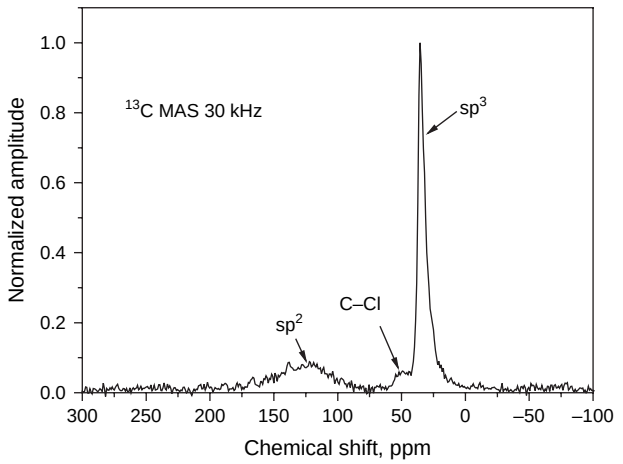

Figure 2. ^{13}C MAS spectrum of Cl-DND (spinning rate 30 kHz, 40 000 scans, recycle delay 2 s).

of the nanodiamond surface accounts for ~24% of all carbons at 800 °C. Similar nanodiamond surface reconstruction into graphitic domains obtained in the XPS study has recently been reported by Petit et al.[37] and Panich et al.[36,38]

The ^{13}C nuclear spin-lattice relaxation measurements for carbons corresponding to the diamond core, at the peak of 35 ppm, reveal that the magnetization recovery is well described by a stretched exponential

$$M(t) = M_{\infty}\left\{1 - \exp\left[-\left(\frac{t}{T_1}\right)^{\alpha}\right]\right\} \qquad (1)$$

where M_{∞} is the equilibrium magnetization, $T_1 = 220 \pm 10$ ms is the spin-lattice relaxation time, and $\alpha = 0.66 \pm 0.03$. The anomalous reduction in the ^{13}C spin-lattice relaxation time from several hours in natural diamond[32,39–41] to 220 ms in Cl-DND, and the stretched exponential character of the magnetization recovery are attributed to the interaction of nuclear spins with unpaired electron spins of paramagnetic defects (in the case in question, broken bonds) observed in EPR measurements.[12–14,16–24] We note that the stretched exponential relaxation is a widely used approach that fits relaxation processes in systems with a number of different relaxation environments. Here the stretched exponential relaxation appears due to a distribution of the nuclear spin-lattice relaxation times in a system of nuclear spins fixed at different distances from the paramagnetic centers.[18,42] The theory of such relaxation[18,42–44] shows that the parameter $\alpha = 1$ is typical for the case of rapid nuclear spin diffusion, while in the regime of vanishing spin-diffusion its value is between 0.5 and 1.[18,42,44] Spin diffusion is driven by the dipole–dipole interaction causing mutual flips of adjacent nuclear spins. Such process should be slow in the case of ^{13}C nuclear spins in nanodiamonds due to low natural abundance (1.1%) of the ^{13}C isotope (the only carbon isotope having nuclear spin) that makes the compound a dilute system with respect to nuclear spins.[18,21,42] This is reflected in the experimentally obtained value of $\alpha = 0.66$.

Well-purified nanodiamonds with the density of paramagnetic defects of $N_s = 6.3 \times 10^{19}$ spins/g[20] exhibit T_1 around 500 ms,[12,13,18,21–25,42] while the Cl-DND sample under study show twice shorter $T_1 = 220$ ms. This finding correlates well with the twice larger density of paramagnetic centers in Cl-DND ($N_s = 1.44 \times 10^{20}$ spin/g) compared with that in initial DND, readily supporting the spin-lattice relaxation mechanism via paramagnetic defects. Similar situation was observed by us in fluorinated DND.[13]

Next, the surface sp^2 carbons show $T_1 = 80 \pm 14$ ms, i.e., faster spin-lattice relaxation compared with that for the carbons of the diamond core. This finding supports our structural model of diamond nanoparticle,[18,21] in which paramagnetic centers are positioned somewhat closer to the DND surface rather than to the center of the core and therefore cause stronger electron-nuclear interaction with

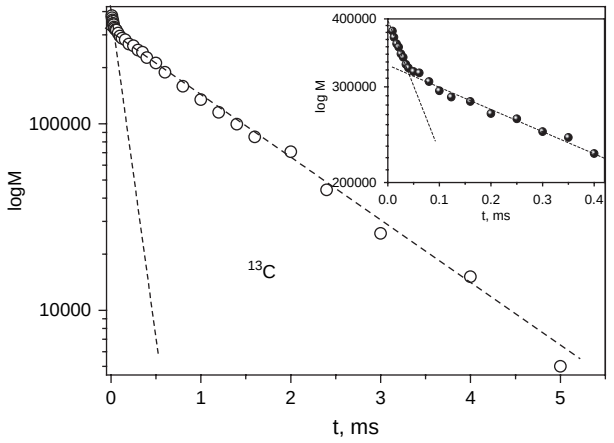

Figure 3. Decay of ^{13}C spin echo amplitude (T_2 measurements) in Cl-DND in semi-logarithmic scale. Inset shows initial part of the decay.

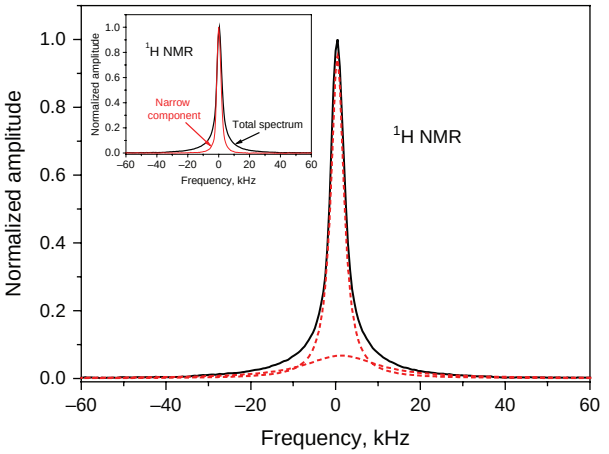

Figure 4. Static ^{1}H spectrum of Cl-DND (320 scans, recycle delay 100 ms). Deconvolution into two components is shown by dashed lines. Inset exhibits both total spectrum and its narrow component measured using dipolar dephasing with delay between pulses 128 μs, when the broad component with shorter T_2 disappears.

the surface and shell carbon spins. One can suggest that these centers are covered by the sp^2-like spots obtained in our experiment, which thus protects them from hydrogen and chlorine termination. On the other hand, they may be positioned in the defected interface shell that covers the nanodiamond core. Anyhow increase in the density of the paramagnetic defects under chlorination points out the specific role of chlorine atoms in breaking the C—C covalent bonds at the diamond surface and in creation new, additional dangling bonds with uncoupled electron spins.

The ^{13}C spin–spin relaxation time (T_2) measurement of the Cl-DND sample shows that the semi-logarithmic plot of the echo amplitude decay consists of at least two linear segments (Fig. 3), and the echo decay may be well fitted by a superposition of two exponentials:

$$M(t) = M_1(0)\exp\left(-\frac{t}{T_{21}}\right) + M_2(0)\exp\left(-\frac{t}{T_{22}}\right) \quad (2)$$

This fact indicates existence of at least two types of carbons with the values of $T_{21} = 0.24 \pm 0.15$ and $T_{22} = 2.48 \pm 0.17$ ms. The longer T_2 (i.e., T_{22}) is attributed to carbons of the diamond core, since these carbons spins experience relatively weak nuclear dipole–dipole interactions owing to low natural abundance of ^{13}C isotopes. The spin–spin relaxation of surface carbon spins (T_{21}) is much faster due to their stronger dipole–dipole coupling with hydrogen and chlorine spins.

3.2. ^{1}H NMR Spectra and Relaxation

High temperature annealing was shown to result in formation of the carboxyl (–COOH) groups by oxidation of the surface carbon atoms and hydrocarbon groups,[11, 36] and to progressive removal of O—H groups with annealing temperature.[26, 36] However, hydrogen atoms at the Cl-DND surface still become apparent in the ^{1}H NMR measurements. Static ^{1}H NMR spectrum (Fig. 4) is well deconvoluted into two lines, a broad component with a line width $\Delta\nu = 21.1$ kHz and a narrow component with $\Delta\nu = 3.6$ kHz, respectively. The former is attributed to the residual closely set hydrocarbon and hydroxyl groups, while the narrow component is assigned to the moisture adsorbed on the DND surface. This assignment results from the hydrophilicity of the DND surface[18] and from the significant reduction of the intensity of the narrow component after pumping out the sample.[11, 15–19]

Existence of two groups of hydrogen atoms is also reflected in the spin–spin relaxation measurements, which are well fit by two exponentials (Fig. 5) with $T_{21} = 0.039 \pm 0.003$ ms and $T_{22} = 0.389 \pm 0.019$ ms. Spin-lattice relaxation measurements show $T_1(^1\text{H}) = 11.64 \pm 0.5$ ms.

^{1}H MAS spectrum of Cl-DND (Fig. 6) is well deconvoluted into two components with chemical shifts of $\sigma =$ 3.23 and 8.97 ppm. The weak signal at 3.23 ppm is assigned to the residual C—H and C—OH groups on the ND surface, while the intense signal at 8.97 ppm

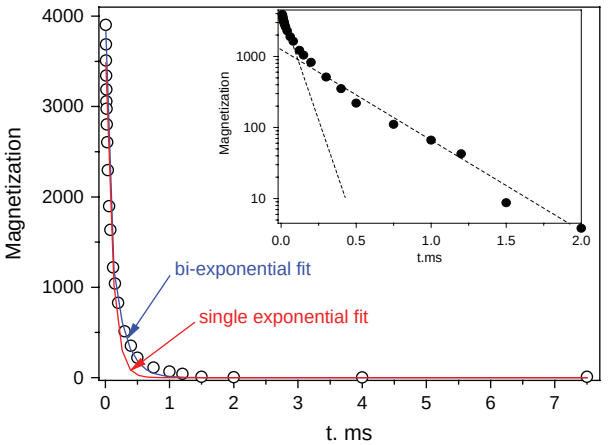

Figure 5. Decay of ^{1}H spin echo amplitude (T_2 measurements) in linear and semi-logarithmic (inset) scales in the Cl-DND. Red and blue lines show single- and bi-exponential fit, respectively.

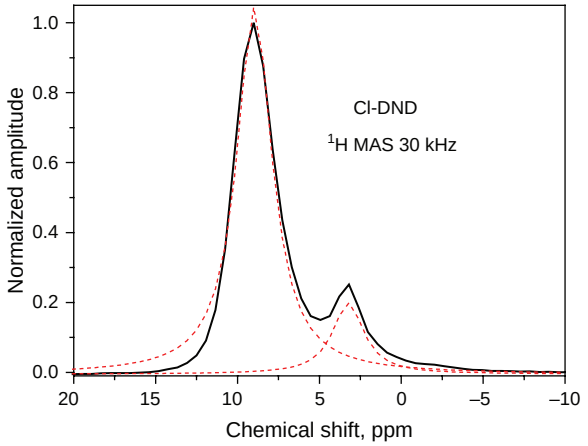

Figure 6. ^{1}H MAS NMR spectrum of Cl-DND measured with spinning rate 30 kHz (100 scans, recycle delay 100 ms). Deconvolution into two components is shown by dashed lines.

is attributed to adsorbed moisture and –COOH groups. We note that the chemical shift of this component differs from that of bulk water and of water molecules adsorbed on the initial nanodiamond surface, $\sigma = 4.76$ ppm and 5.8–6 ppm, respectively.[36] This deviation may reflect the proton exchange between carboxyl group (whose shift varies between 9 to 13 ppm[45]) and adsorbed water molecules.[11] Such a process is characteristic of carboxyl groups involved into chemical exchange, whose spectrum usually occurs as a singlet with exact chemical shift depending on the actual content of water molecules.

3.3. ^{35}Cl NMR Spectrum

Chlorinated nanodiamond under study contains around 4% of chlorine (Table I). ^{35}Cl isotope has nuclear spin $I = 3/2$ and possesses quadrupole moment of $Q(^{35}\mathrm{Cl}) = -0.0855$ b, thus it is sensitive to the electric field gradient that arises at a nuclear site of a non-cubic symmetry. The quadrupolar contribution gives rise to a large line width of the powder spectra. The low concentration of chlorine in the nanodiamond sample under study, low resonant frequency for ^{35}Cl isotope, and large line width result in the low ^{35}Cl signal intensity. Therefore the ^{35}Cl NMR spectrum (Fig. 7) is represented by a weak broad line. The observed ^{35}Cl chemical shift of ~580 ppm (relative to 0.1 mol solution of NaCl in D_2O at 0 ppm) is in the range typical of covalent C—Cl bonds.[46] This finding confirms that chlorine is indeed bound to the nanodiamond surface. Spectrum simulation yields room temperature ^{35}Cl quadrupolar frequency $\nu_Q \approx 24$ MHz and asymmetry parameter $\eta \approx 1$. The value of ν_Q lies close to the range of chlorine quadrupolar frequencies in organic compounds with covalent C—Cl bonds, 27–40 MHz.

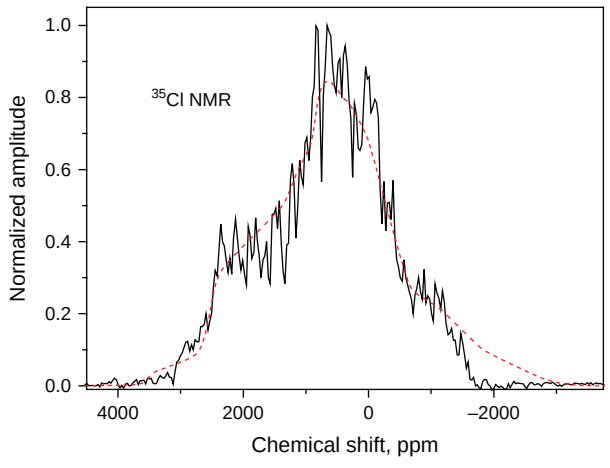

Figure 7. Experimental room temperature ^{35}Cl NMR spectrum of Cl-DND at resonance frequency 33.38 MHz (black continuous line, 3200000 scans, recycle delay 100 ms) and the calculated spectrum (red dash line) for $\nu_Q = 24$ MHz and $\eta = 1$.

3.4. XPS Spectra

XPS measurement of the Cl-DND sample reveals the surface composition as 93.3 at.% of carbon, 2.28 at.% of oxygen and 4.41 at.% of chlorine atoms. Figure 8(a) shows the C 1 s spectrum that is deconvoluted into three lines

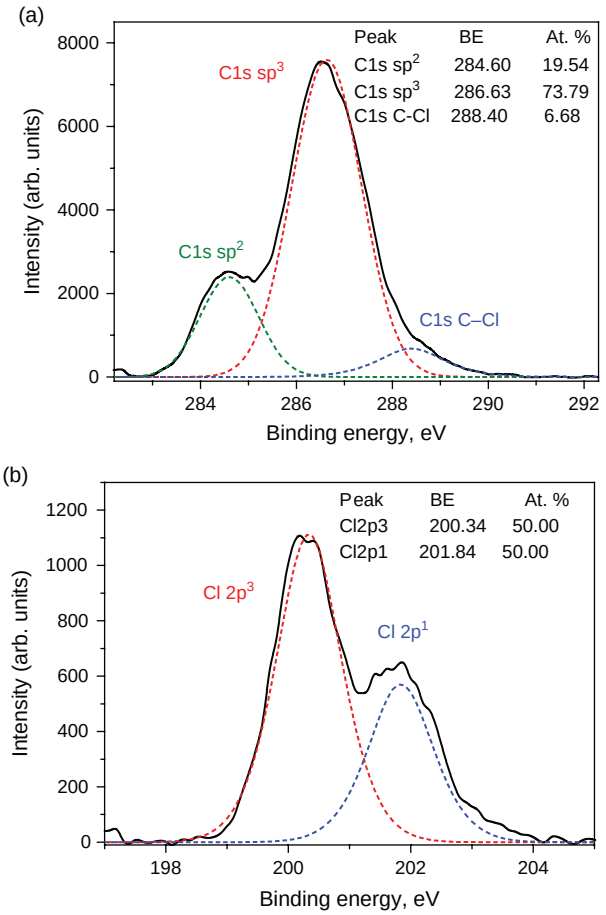

Figure 8. (a) Carbon 1*s* and (b) chlorine 2 *p* XPS spectra of Cl-DND. Deconvolutions into (a) three and (b) two components are shown by dashed lines.

assigned to three kinds of carbon atoms. Here the dominant C 1*s* peak with the binding energy 286.6 ± 0.2 eV was definitely assigned to the sp^3 carbons of the diamond core[47–53] that embodies most of the carbon atoms. The weaker peaks showing binding energies of 284.6 ± 0.2 eV and 288.4 ± 0.2 eV are attributed to sp^2 carbons and to carbon atoms forming C—Cl bonds, respectively.[47–53] We note that carbon atoms involved in carbon—halogen bonds usually show larger binding energies compared to those of non-halogenated carbons.[53]

The chlorine 2*p* XPS spectrum (Fig. 8(b)) reveals a C1 2*p*3 peak centered around 201 eV, which corresponds to the C—Cl bonds.[53] This finding is in accordance with the aforementioned C 1*s* XPS and NMR data. The peak results from chlorine 2*p* electrons, and its shape is governed by the spin split of the electrons of 2*p* level.

4. CONCLUSION

We have carried out a combined ^{1}H, ^{13}C and ^{35}Cl NMR and XPS investigation of the structure and chemical bonding in detonation nanodiamond annealed at 800 °C in chlorine atmosphere. This study leads to conclusion that the hydrocarbon and hydroxyl groups are partially removed from the DND surface in the process of chlorination and substituted by chemically active chlorine atoms, resulting in the occurrence of the chlorine-carbon groups on the DND surface. The annealing at 800 °C also results in a partial graphitization of the diamond surface and appearance of a sp^2-like carbon shell. Chlorine atoms are covalently bound to the carbon atoms at the surface of the nanoparticles. Interaction between paramagnetic centers (uncoupled electron spins of broken bonds) and nuclear spins results in fast ^{13}C nuclear spin-lattice relaxation.

Acknowledgment: This work was supported by New Energy Development Organization of Japan Grant No. 04IT4, joint grant of the Israeli Ministry of Science and Technology and Russian Foundation for Basic Research No. 3-5708, and partially by the grant of the Israeli Ministry of Science and Technology No. 3-9754. Alexander Ya. Vul' and Arthur T. Dideykin thank for support the Program N 24 of Presidium of the Russian Academy of Sciences. We thank A. Shames for the EPR measurement of paramagnetic centers content and useful discussion.

References and Notes

1. A. M. Schrand, S. A. Ciftan Hens, and O. A. Shenderova, *Crit. Rev. Solid State and Mater. Sci.* 34, 18 (**2009**).
2. V. Yu. Dolmatov, *Russ. Chem. Rev.* 76, 339 (**2007**).
3. A. S. Barnard, *Analyst* 134, 1751 (**2009**).
4. M. Baidakova and A. Vul', *J. Phys. D: Appl. Phys.* 40, 6300 (**2007**).
5. V. N. Mochalin, O. Shenderova, D. Ho, and Yu. Gogotsi, *Nature Nanotechnol.* 7, 11 (**2012**).
6. M. Terranova, S. Orlanducci, and M. Rossi, Carbon Nanomaterials for Gas Adsorption, Pan Stanford Publishing, Singapore (**2012**), p. 494.
7. V. Guglielmotti, S. Chieppa, S. Orlanducci, E. Tamburri, F. Toschi, M. L. Terranova, and M. Rossi, *Appl. Phys. Lett.* 95, 222113 (3pp) (**2009**).
8. D. Ho (ed.), Nanodiamonds: Applications in Biology and Nanoscale Medicine, Spinger, Dordrecht, Heidelberg, New York, London (**2010**).
9. O. A. Williams, J. Hees, C. Dieker, W. Jager, L. Kirste, and C. E. Nebel, *ACS Nano* 4, 4824 (**2010**).
10. A. E. Aleksenskiy, E. D. Eydelman, and A. Ya. Vul', *Nanosci. Nanotechnol. Lett.* 3, 68 (**2011**).
11. A. M. Panich and A. E. Aleksenskii, *Diamond Relat. Mater.* 27, 45 (**2012**).
12. A. M. Panich, A. I. Shames, O. Medvedev, V. Yu. Osipov, A. E. Alexenskii, and A. Ya. Vul', *Appl. Magn. Reson.* 36, 317 (**2009**).
13. A. M. Panich, H.-M. Vieth, A. I. Shames, N. Froumin, E. Ōsawa, and A.Yao, *J. Phys. Chem. C* 114, 774 (**2010**).
14. A. I. Shames, A. M. Panich, V. Yu. Osipov, A. E. Aleksenskiy, A. Ya. Vul', T. Enoki, and K. Takai, *J. Appl. Phys.* 107, 014318 (**2010**).
15. O. Shenderova, A. M. Panich, S. Moseenkov, S. C. Hens, V. L. Kuznetsov, and H.-M. Vieth, *J. Phys. Chem. C* 115, 19005 (**2011**).
16. A. M. Panich, A. Altman, A. I. Shames, V. Yu. Osipov, A. E. Alexenskiy, and A. Ya. Vul', *J. Phys. D: Appl. Phys.* 44, 125303 (5pp) (**2011**).
17. A. M. Panich, H.-M. Vieth, and O. Shenderova, *Fullerenes, Nanotubes and Carbon Nanostruct.* 20, 579 (**2012**).
18. A. M. Panich, *Crit. Rev. Solid State Mater. Sci.* 37, 276 (**2012**).
19. A. M. Panich, A. I. Shames, B. Zousman, and O. Levinson, *Diamond Relat. Mater.* 23, 150 (**2012**).
20. V. Yu. Osipov, A. I. Shames, T. Enoki, K. Takai, M. V. Baidakova, and A. Ya. Vul', *Diamond Relat. Mater.* 16, 2035 (**2007**).
21. A. M. Panich, A. I. Shames, H.-M. Vieth, E. Ōsawa, M. Takahashi, and A. Ya. Vul', *Europ. Phys. J. B* 52, 397 (**2006**).
22. A. I. Shames, A. M. Panich, W. Kempiński, A. E. Alexenskii, M. V. Baidakova, A. T. Dideikin, V. Yu. Osipov, V. I. Siklitski, E. Osawa, M. Ozawa, and A. Ya. Vul', *J. Phys. Chem. Solids* 63, 1993 (**2002**).
23. A. I. Shames, A. M. Panich, W. Kempiński, M. V. Baidakova, V. Yu. Osipov, T. Enoki, and A. Ya. Vul', Magnetic resonance study of nanodiamonds, Synthesis, Properties and Applications of Ultrananocrystalline Diamond, edited by D. M. Gruen, O. A. Shenderova, and A. Ya. Vul', NATO Science Series II, Springer, Dordrecht, Netherlands (**2005**), Vol. 192, pp. 271–282.
24. G. Cunningham, A. M. Panich, A. I. Shames, I. Petrov, and O. Shenderova, *Diamond Relat. Mater.* 17, 650 (**2008**).
25. A. M. Panich, *Diamond Relat. Mater.* 16, 2044 (**2007**).
26. V. Mochalin, S. Osswald, and Y. Gogotsi, *Chem. Mater.* 21, 273 (**2009**).
27. A. E. Aleksenskii, M. V. Baidakova, A. Ya. Vul', V. Yu. Davidov, and Yu. A. Pevtsova, *Phys. Solid State* 39, 1007 (**1997**).
28. S. Osswald, G. Yushin, V. Mochalin, S. O. Kucheyev, and Y. Gogotsi, *J. Am. Chem. Soc.* 128, 11635 (**2006**).
29. J. C. Arnault, S. Saada, M. Nesladek, O. A. Williams, K. Haenen, P. Bergonzo, and E. Osawa, *Diamond Relat. Mater.* 17, 1143 (**2008**).
30. G. Lisichkin, V. Korol'kov, B. Tarasevich, I. Kulakova, and A. Karpukhin, *Russ. Chem. Bull.* 55, 2212 (**2006**).
31. T. M. Duncan, *J. Phys. Chem. Ref. Data* 16, 125 (**1987**).
32. M. J. Duijvestijn, C. van der Lugt, J. Smidt, R. A. Wind, K. W. Zilm, and D. C. Staplin, *Chem. Phys. Lett.* 102, 25 (**1983**).
33. H. L. Retcofsky and R. A. Friedel, *J. Phys. Chem.* 77, 68 (**1973**).
34. A. M. Panich, *Synth. Metals* 100, 169 (**1999**).
35. Leah B. Casabianca, Alexander I. Shames, Alexander M. Panich, Olga Shenderova, and Lucio Frydman, *J. Phys. Chem. C* 115, 19041 (**2011**).
36. A. M. Panich, A. I. Shames, N. A. Sergeev, M. Olszewski, J. K. McDonough, V. Mochalin, and Y. Gogotsi, *J. Phys.: Condens. Matter* 25, 245303 (8pp) (**2013**).
37. T. Petit, J.-C. Arnault, H. A. Girard, M. Sennour, and P. Bergonzo, *Phys. Rev. B* 84, 233407 (**2011**).

38. A. M. Panich, A. I. Shames, N. A. Sergeev, M. Olszewski, V. Mochalin, and Y. Gogotsi, Nanodiamond-to-onion transformation—A magnetic resonance study, *Intern. Conf. Diamond and Carbon Materials (Diamond-2013)*, Programme Book, Abstract O-004, Riva del Garda, Italy. September **(2013)**.
39. M. J. R. Hoch and E. C. Reynhardt, *Phys. Rev. B* 37, 9222 **(1988)**.
40. E. C. Reynhardt and C. J. Terblanche, *Chem. Phys. Lett.* 269, 464 **(1997)**.
41. C. J. Terblanche, E. C. Reynhardt, and J. A. vanWyk, *Chem. Phys. Lett.* 310, 97 **(1999)**.
42. A. M. Panich and G. B. Furman, *Diamond Relat. Mater.* 23, 157 **(2012)**. Corrigendum: *ibid.* 29, 1 **(2012)**.
43. W. E. Blumberg, *Phys. Rev.* 119, 79 **(1960)**.
44. G. B. Furman, A. M. Panich, A. Yochelis, E. M. Kunoff, and S. D. Goren, *Phys. Rev. B* 55, 439 **(1997)**.
45. H. Günther, NMR Spectroscopy, John Willey and Sons, Chichester **(1980)**.
46. R. P. Chapman, C. M. Widdifield, and D. L. Bryce, *Progr. Nucl. Magn. Resonan. Spectrosc.* 55, 215 **(2009)**.
47. Y. Liu, Z. Gu, J. L. Margrave, and V. N. Khabashesku, *Chem. Mater.* 16, 3924 **(2004)**.
48. J. W. Robinson (ed.), Practical Handbook of Spectroscopy, CRC Press, Boston **(1991)**.
49. T. Nakajima, M. Koh, R. N. Singh, and M. Shimada, *Electrochim. Acta* 44, 2879 **(1999)**.
50. T. Nakajima, Synthesis, structure, and physicochemical properties of fluorine-graphite intercalation compounds, Fluorine-Carbon and Fluoride-Carbon Materials, edited by T. Nakajima, Marcel Dekker, NY **(1995)**.
51. T. Nakajima, V. Gupta, Y. Ohzawa, M., Koh, R. N. Singh, A. Tressaud, and E. Durand, *J. Power Sources* 104, 108 **(2002)**.
52. Yu. V. Lavskaya, L. G. Bulusheva, A. V. Okotrub, N. F. Yudanov, D. V. Vyalikh, and A. Fonseca, *Carbon* 47, 1629 **(2009)**.
53. T. I. T. Okpalugo, P. Papakonstantinou, H. Murphy, J. McLaughlin, and N. M. D. Brown, *Carbon* 43, 153 **(2005)**.

Received: 7 June 2013. Accepted: 3 January 2014.